Quantifying the Likelihood of Substructure in Coronal Loops

Kathryn McKeough[1]

Vinay Kashyap[2], Sean McKillop[2], David van Dyk[3], Nathan Stein[4]

(1) Carnegie Mellon University, Pittsburgh, PA; (2) Harvard-Smithsonian Center for Astrophysics, Cambridge, MA ; (3) Imperial College London, United Kingdom; (4) University of Pennsylvania, Phillidelphia PA

Goal

To develop a method to search for substructure in solar images. By identifying the substructure of coronal loops, we determine dominant spatial scales and constrain theories of coronal heating.

1. Test for substructure in regions in AIA (green) that have corresponding Hi-C image (yellow)
2. See whether regions in AIA, without a corresponding Hi-C image have similar substructure detections

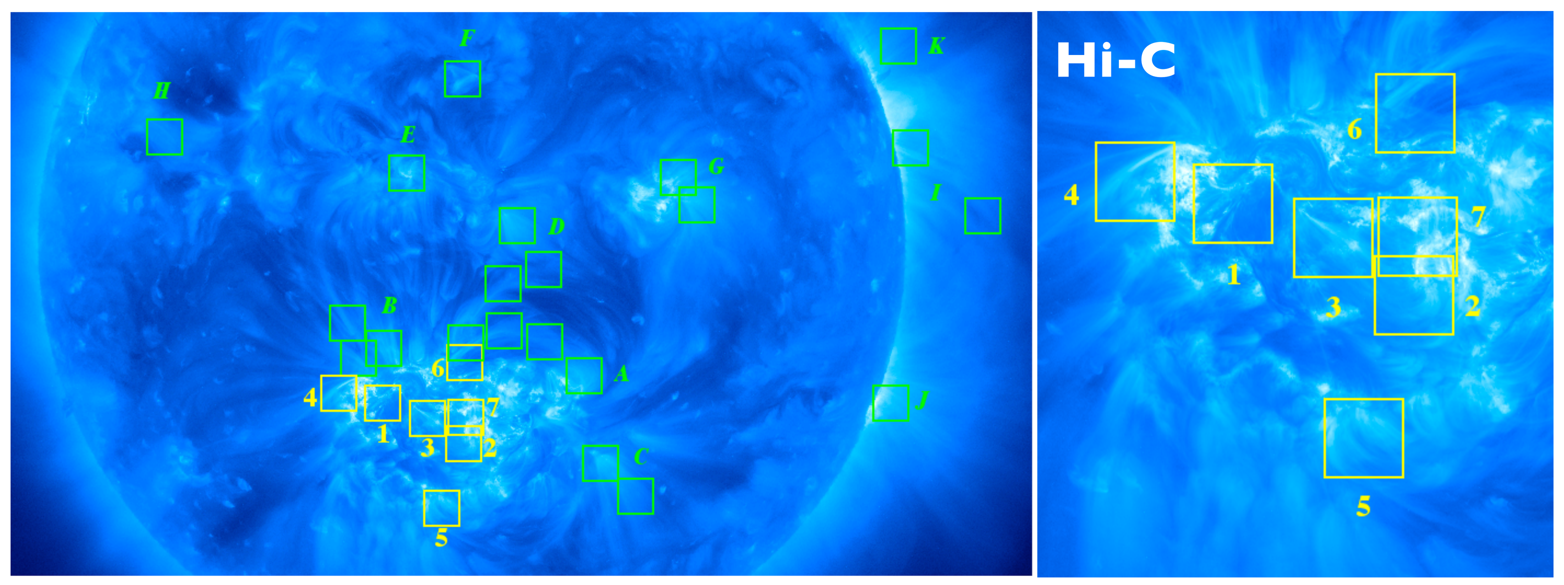

Background

- One of the major unsolved questions in coronal astrophysics is where the energy to heat the corona comes from.
- The **corona** is the outermost layer of the sun and is made up of high-temperature plasma.
- **Coronal loops** are magnetic flux tubes, filled with plasma, that run through the corona and connect regions of opposite magnetic polarity.

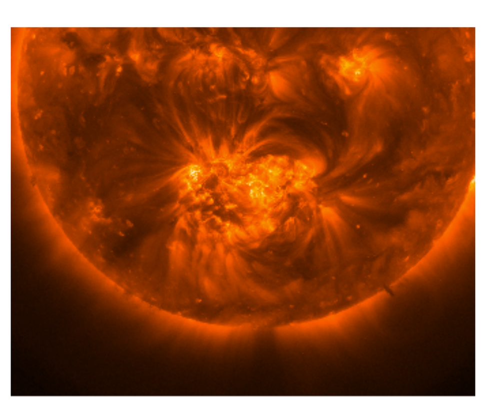

AIA image of Corona[a]

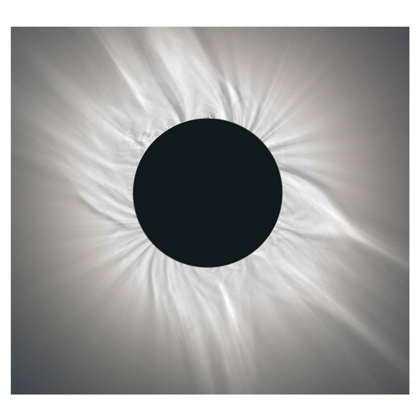

Outer corona during eclipse[b]

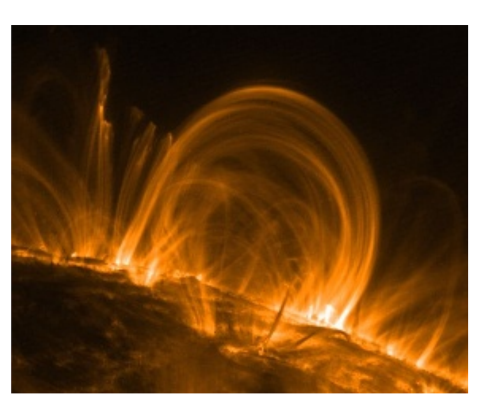

Coronal loop[c]

- **Alfen wave** dissipation is a large-spatial–scale heating mechanism that dissipates energy into the corona through turbulence.
- **Nanoflares** are small-spatial–scale consecutive bursts of energy from magnetic reconnection that contribute to heating and is induced by stresses at the footpoints that cause braided substructure along the loops.

a AIA 193 A 2012/07/11 18:53:44; b http://apod.nasa.gov/apod/ap090726.html; c http://www.daviddarling.info

References & Aknowledgments

Brooks, D. et al. 2013, ApJ, 722L, 19B
Cargill, P., & Klimchuck, J. 2004, ApJ, 605, 911C
Connors, A., & van Dyk, D. A. 2007, Statistical Challenges in Modern Astronomy IV, 371, 101
Cranmer, S., et al. 2012, ApJ, 754, 92C
Cranmer, S., et al. 2007, ApJS, 171, 520C
DeForest, C. E. 2007, ApJ, 661, 532D
Esch, D. N., Connors, A., Karovska, M., & van Dyk, D. A. 2004, ApJ, 610, 1213
Pastourakos, S., & Klimchuk, J. 2005, ApJ, 628, 1023P
Raymond, J. C., et al. 2014, ApJ, 788, 152R
Stein, N., et al. *to be submitted to ApJ*
Viall, N. M., & Klimchuck J. 2011, ApJ, 738, 24V
Wee, C. Y., & Paramesran, R. 2008, ICSP2008 Proceedings, 978-1-4244-2179-4/08

We acknowledge support from AIA under contract SP02H1701R from Lockheed-Martin to SAO.

We acknowledge the High resolution Coronal Imager instrument team for making the flight data publicly available. MSFC/NASA led the mission and partners include the Smithsonian Astrophysical Observatory in Cambridge, Mass.; Lockheed Martin's Solar Astrophysical Laboratory in Palo Alto, Calif.; the University of Central Lancashire in Lancashire, England; and the Lebedev Physical Institute of the Russian Academy of Sciences in Moscow.

VK acknowledges support from NASA Contract to Chandra X-ray Center NAS8-03060

We acknowledge Smithsonian Competitive Grants Fund 40488100HH0043.

We acknowledge the support from the Solar REU program at Harvard Smithsonian CfA.

Increased Spatial Resolution

High-Resolution Coronal Imager (Hi-C) | **Atmospheric Imaging Assembly (AIA)**

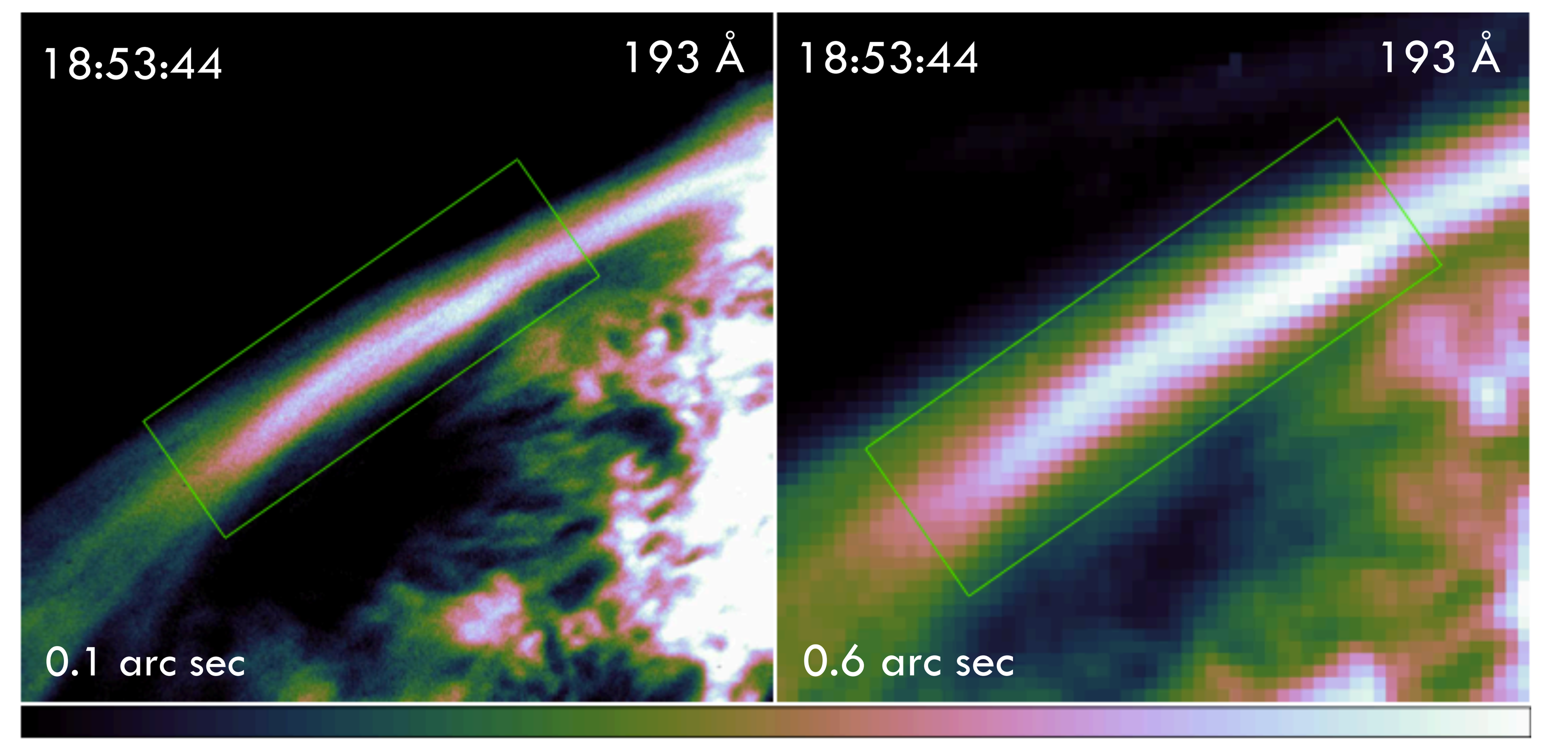

- Hi-C images are at high resolution; it was a rocket flight that recorded a small region of the sun in a short amount of time.
- Some of the loops seen to be "monolithic" in AIA were found to have sub-strands in Hi-C images.
- **Low Count Image and Reconstruction Analysis (LIRA) :**
  - Bayesian and Markov Chain Monte Carlo (MCMC) algorithm
  - Components:
    - *Smoothed underlying baseline*
    - *Inferred multi-scale component*

Sharpness Statistic

$g(x,y)$ →	Image matrix
$\tilde{g}(x,y) = \dfrac{g(x,y)}{\sqrt{\sum_{x=0}^{N-1}\sum_{0}^{N-1}[g(x,y)]^2}}$ →	Normalization
$G = \tilde{g}(x,y) - \mu$ →	Subtract mean
$S_{\tilde{g}} = \dfrac{1}{(N-1)} GG^T$ →	Covariance matrix
$S_{\tilde{g}} = UDV$ →	Singular Value Decomposition
$\sum^{N} \lambda^2 = \psi$ →	Sum of squared eigenvalues (diagonal of *D*)

- **Sharpness** (ψ) quantifies the prominence of the substructure (Wee & Paramesran 2008) using the sum of the eigenvalues of the covariance matrix
- Slide a 5x5 window across LIRA output to calculate sharpness at each location.

(Left) LIRA multi-scale component
(Right) Each pixel in the sharpness image corresponds to a 5x5 window in the LIRA image. The brighter the pixel, the more features present in the window.

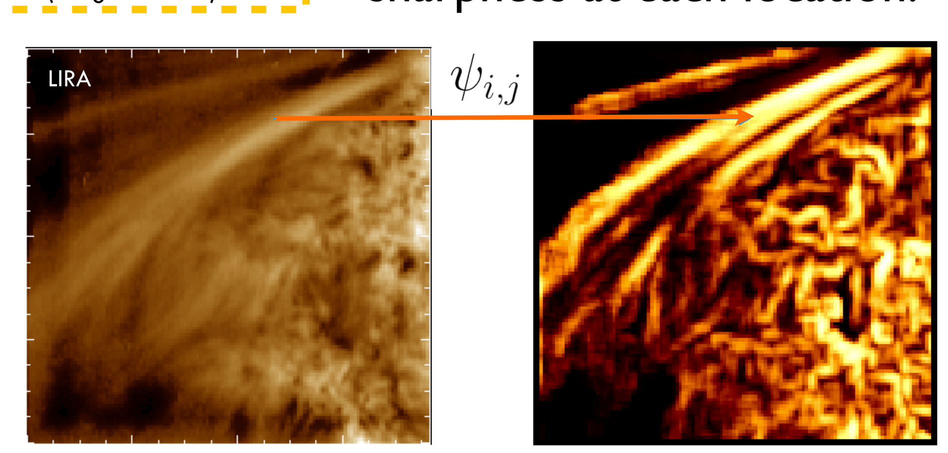

Gradient Correction

- Sharpness is sensitive to edges due to dramatic gradient changes.
- The gradient correction makes data independent of gradient change.
- A regression line is fit on sharpness with gradient in log-log space
- The correction is made by pivoting the points about the mean to make the best fit slope horizontal
- This is done independently for every image.

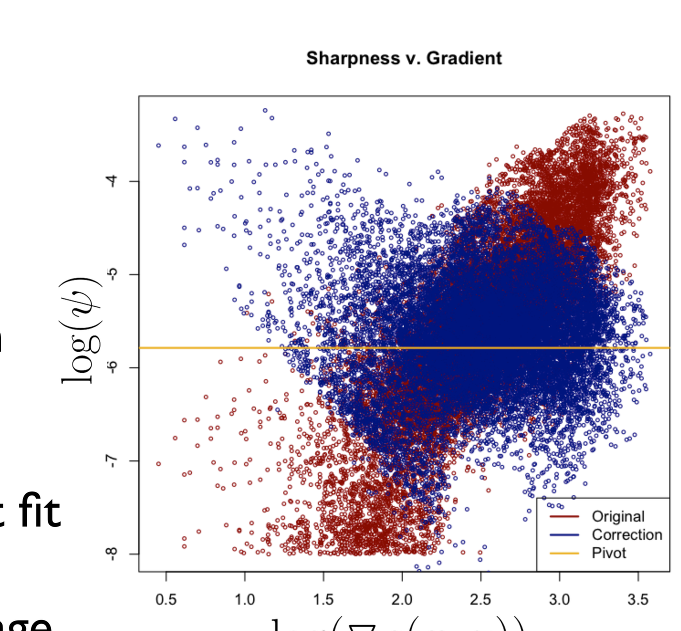

Significance Test

- Compare observation to image drawn from the "null hypothesis", that no substructure is present in the coronal loops.
- The null image is created by convolving the observed image with the point spread function to remove structure at pixel resolution.
  - The null distribution is created using MCMC iterations of 5 Poisson realizations of the null image.
  - The alternative (observed) distribution is created from MCMC iterations of observed image.
- We compare the corrected sharpness values of the null distribution and alternative distribution using the **p-value upper bound** ($\hat{u}$).

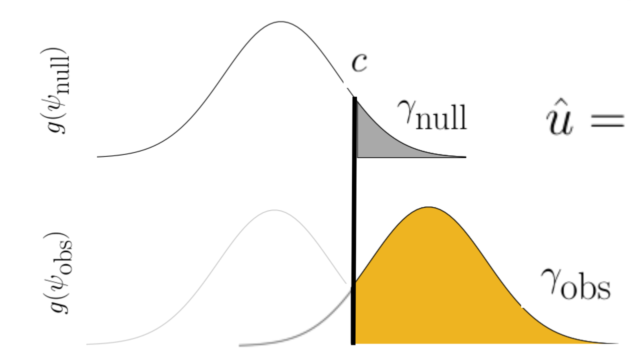

$$\hat{u} = \frac{\gamma_{\text{null}}}{\gamma_{\text{obs}}}$$

$g(\psi)$	probability distribution of sharpness
γ_{null}	probability having a sharpness greater than or equal to *c* from null distribution
c	threshold determined by $\gamma_n = 0.005$
γ_{obs}	probability having a sharpness greater than or equal to *c* from observed distribution

Results

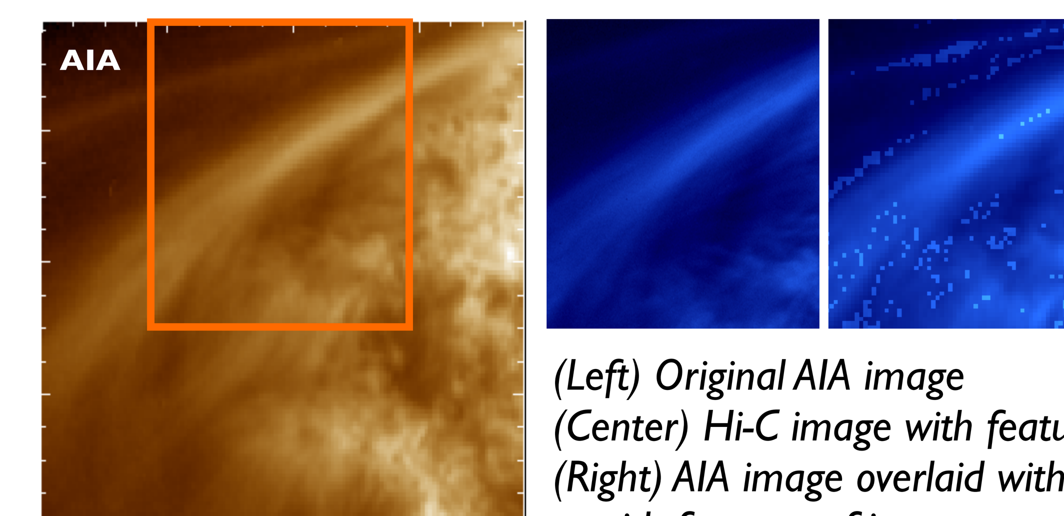

(Left) Original AIA image
(Center) Hi-C image with features of interest marked
(Right) AIA image overlaid with significant, highlighted pixels with features of interest marked

- A Significance test is performed for each pixel in AIA image.
- We compare results to Hi-C for proof of concept.

- The same analysis was applied to images outside of the Hi-C region, taken from different areas of the corona.
- Most loops showed non-detections

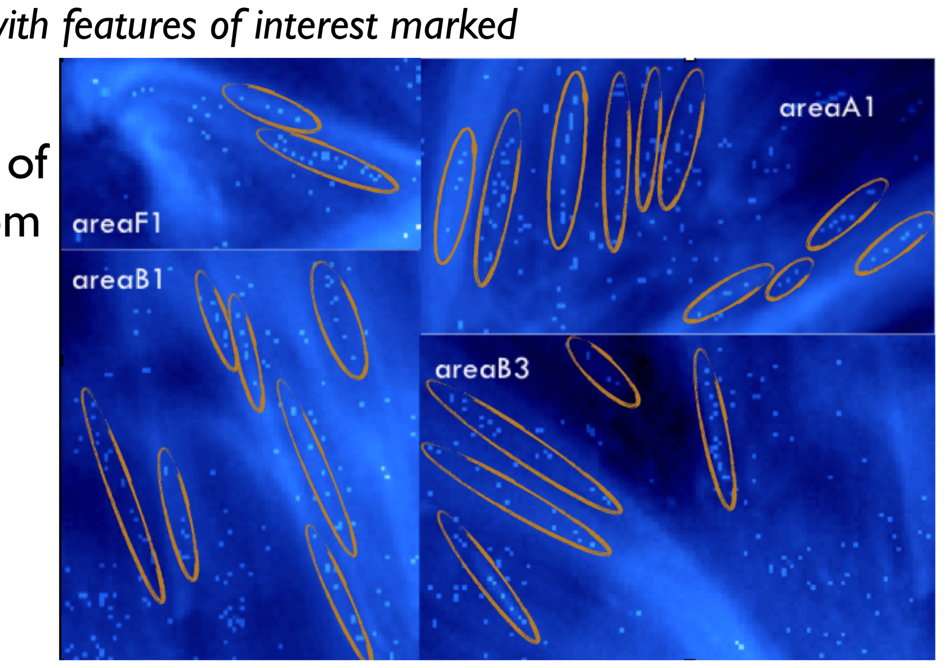

Images where substructure was detected with features marked

Discussion & Conclusion

- We have adapted LIRA to work on extended sources.
- We find that in every instance that the AIA loop is known to be resolvable, our algorithm recognizes it as such.
- Applying the algorithm to areas on the Sun that were not covered by Hi-C, we find that loops with substrands are ubiquitous.
- Not all loops are found to have substructure, and isolated points suggest result of Poisson artifacts.

Future Work

- Results are preliminary:
  - Quantify false positive and non-detections
  - Increasing power of test could expand detection regions
- Understand the implications:
  - Relation between bright points and detections compare light curves of significant pixels
  - Why some loop complexes show no significant detections